Double Critical Phenomena in (Water + Polyacrylamides) Solutions

**L. P. N. Rebelo,*,† Z. P. Visak,† H. C. de Sousa,‡ J. Szydlowski,†,#
R. Gomes de Azevedo,† A. M. Ramos,§ V. Najdanovic-Visak,†
M. Nunes da Ponte,† and J. Klein⊥**

*Instituto de Tecnologia Química e Biológica, ITQB 2, Universidade Nova de Lisboa, Av. República,
Apartado 127, 2780-901 Oeiras, Portugal; Departamento de Engenharia Química, Universidade de
Coimbra, Polo II, Pinhal de Marrocos, 3030 Coimbra, Portugal; Departamento de Química e CQFB,
Faculdade de Ciências e Tecnologia da UNL, 2825-114 Caparica, Portugal; and Lehrstuhl für
Makromolekulare Chemie, Technische Universität Braunschweig, Hans-Sommer-Str. 10 D-38106
Braunschweig, Germany*

ABSTRACT: Aqueous solutions of a copolymer derivative of a polyacrylamide showed very interesting behavior, that in which the system evolves from one kind of double criticality (pressure−hypercritical point) to another (temperature−hypercritical point) as polymer molecular weight decreases. While in the neighboring region of the former point one expects a change from contraction to expansion upon mixing with increasing pressure; in the latter, mixing should be accompanied by a change in the sign of the excess enthalpy as temperature increases. L−L equilibria studies were performed in a wide range of (T, p) experimental conditions ($300 < T/\mathrm{K} < 460$, $0 < p/\mathrm{bar} < 700$). Poly(N-isopropylacrylamide), usually called PNIPAAM, and its copolymer derivative poly(N-isopropylacrylamide/1-deoxy-1-methacrylamido-D-glucitol), herein referred to as CP, were investigated for several chain lengths and compositions. An He/Ne laser light scattering technique was used for the determination of cloud-point (T, p, x) conditions. The experimental results were used to assist in the determination of computed values at temperatures beyond experimental accessibility, which are obtained by the application of a modified Flory−Huggins model. The model also estimates the excess properties of these solutions. Because of the intrinsic self-associating nature of these systems, all studied solutions show a lower critical solution temperature (LCST). Both modeling results and H/D isotope substitution effects suggest also the existence of upper critical solution temperatures (UCST) and therefore closed-loop-type phase diagrams. However, these upper-temperature branches are experimentally inaccessible. Pressure effects are particularly interesting. For a low-MW CP, experimental data display a tendency toward a reentrant $T-p$ locus, which supports the conjecture that these systems are inherently of the closed-loop type. In the cases of PNIPAAMs and high-MW CPs, the $T-p$ isopleths show extrema. The copolymer aqueous solutions under study in this work model a single chemical system where pressure−hypercritical behavior evolves to a temperature−hypercritical one as the chain length decreases.

1. Introduction

Room temperature water-soluble polymers such as poly(N-isopropylacrylamide), the so-called PNIPAAM, and its copolymer derivatives have received increasing attention during recent years,[1−6] in both academic and industrial contexts. This is mainly due to the large number of their possible applications.[1,2] However, there is still a lack of accurate phase equilibria and thermodynamic experimental data for these aqueous systems.

Because of the intrinsically strong orientation-dependent nature of intermolecular forces in these solutions, experimentally observed phase transitions occur at the lower critical solution temperature (LCST) curve. The (p, T, x) conditions of its occurrence is governed by the interplay between hydrophilic and hydrophobic interactions. Consequently, our interest not merely focused on PNIPAAM but also on one of its hydrophilically modified copolymers,[7] the poly(N-isopropylacrylamide/1-deoxy-1-methacrylamido-D-glucitol), referred to herein simply as CP. In a previous preliminary study

of these types of systems[8] we speculated, on the basis of solvent isotope (H/D) effect studies, that these solutions might also show, at high temperatures, an upper critical solution temperature (UCST) branch. Thus, the corresponding phase diagram is inherently of the closed-loop type in its (T, x) projection, although the upper branch cannot be easily reached experimentally. In contrast with PNIPAAM, about which several authors[1,3,5,6] have correctly claimed that phase transitions of its aqueous solutions are reasonably independent of molecular weight (MW) and concentration, solutions of CP may behave differently. Here, the substitution of some isopropylacrylamide monomeric segments by vinylsaccharidic ones permits better solubility, shifting LCST transitions to higher temperatures. Thus, laboring under the assumption that UCST transitions should also be present at high temperatures, an increase in vinylsaccharide content in the polymer will shrink the two-phase (T, x) region of the closed loop toward a single point (double critical point). In the neighboring region of this point (hypercritical region), several properties should change markedly. Significant molecular weight and composition effects are thus expected to occur.

The experimental technique for detecting phase transitions uses the increase of scattered light and the simultaneous decrease of the transmitted one that results from lighting the sample with an He−Ne laser

† Universidade Nova de Lisboa.
‡ Universidade de Coimbra.
§ Faculdade de Ciências e Tecnologia da UNL.
⊥ Technische Universität Braunschweig.
Permanent address: Chemistry Department, Warsaw University, Zwirki I Wigury 101, 02-089 Warsaw, Poland.
* Corresponding author. E-mail luis.rebelo@itqb.unl.pt.

Table 1. Polymer Characteristics (PNIPAAM = Poly(*N*-isopropylacrylamide); VS = 1-Deoxy-1-methacrylamido-D-glucitol)

sample	polymer	VS content (mol %)	$[\eta]$ (mL g^{-1})	$\bar{M}_w \times 10^{-5}$	$\bar{M}_w/\bar{M}_n$
P1	PNIPAAM		62.7	6.15	2.04
P2	PNIPAAM		40.6	2.58	2.15
P3	PNIPAAM		30.3	1.44	2.06
CP1	copoly(PNIPAAM/VS)	14.0	56.1	4.32	2.97
CP2	copoly(PNIPAAM/VS)	12.9	16.2	1.70	2.18
CP3	copoly(PNIPAAM/VS)	13.7	1.02	1.10	2.13
CP4	copoly(PNIPAAM/VS)	13.3	0.38	0.56	1.96

beam as the solution undergoes phase separation. A detailed explanation of the methodology can be found elsewhere.[9] In the current work, we also used a modified version of that methodology in order to both achieve higher pressures (up to 700 bar) and better turbidity contrast (see Experimental Section).

To better understand the nature of the equilibria involved, a modified Flory−Huggins model[10−12] was employed. Computed results extend the phase diagrams to experimentally inaccessible regions and provide information on the excess properties of these mixtures.[13]

2. Experimental Section

A. Polymer Synthesis and Characterization. The homopolymer poly(*N*-isopropylacrylamide) and several copolymers with an attached vinylsaccharidic label (see Figure 1), referred to as copoly(PNIPAAM/VS) or simply CP, more precisely copoly(*N*-isopropylacrylamide/1-deoxy-1-methacrylamide-D-glucitol), were synthesized by radical polymerization.

The reactions were carried out in 5 cm^3 magnetically stirred microvials, under a nitrogen atmosphere at 25 °C in an aqueous solution for 24 h, using the redox pair (NH$_4$)$_2$S$_2$O$_8$/Na$_2$S$_2$O$_5$ as a radical initiator. The concentration relationship between the oxidative part of the redox couple ((NH$_4$)$_2$S$_2$O$_8$, concentration 2.0×10^{-2} M) and the reductive part (Na$_2$S$_2$O$_5$, concentration 7.5×10^{-2} M) was maintained constant in all experiments. These concentrations correspond to the values reported in the literature as giving rise to the highest yield on the homopolymerization reaction of 1-deoxy-1-methacrylamido-D-glucitol.[7]

To obtain products with different average molecular weights, copolymerizations were performed using an initial comonomer composition of 10 mol % of vinylsaccharide (VS) and different amounts of radical initiatior, namely 0.2%, 1.0%, 1.5%, and 2.0% (mole percent on monomers). Polymers were purified by ultrafiltration and recovered by freeze-drying.

The vinylsaccharide monomer was previously synthesized according to the literature,[7] by reacting 1-amino-1-desoxy-D-sorbitol (Aldrich Chemical Co.) with methacrylic anhydride (Fluka Chemie AG, Buchs, Switzerland). In the homopolymerization reaction of *N*-isopropylacrylamide (Aldrich Chemical Co.) 0.6, 2.5, and 4.0 mol % of monomer of radical initiator were used (samples P1 to P3, respectively; see Table 1).

The copolymer composition was determined by elemental analysis of C, H, and N. Capillary viscometry in 0.1 M Na$_2$SO$_4$ solution at 25 °C was performed to determine the viscosity limit number. Using static multiangle laser light scattering (Dawn DSP Laser Photometer, Wyatt Tech. Co.), all copolymers were characterized to obtain the weight-average molecular weight, $\bar{M}_w$. Polydispersities, $\bar{M}_w/\bar{M}_n$, were measured by GPC/SEC in a Waters Co. apparatus at 25 °C using water as eluent and a Waters hydrogel linear column. Using monodisperse pullulan standards (Shodex, Showa Denko, Japan, in the molecular weight range 0.59×10^4 to 78.8×10^4), the calibration curve was generated. The characteristics of the polymer samples used in this work are reported in Table 1.

B. Solvents. H$_2$O used in this work was doubly distilled and deionized (Millipore Co. equipment) and stored in sealed microvials. To avoid background turbidity, in all cases and prior to the injection into the light scattering cell, solutions were filtered of suspended impurities.

C. Equipment and Technique. The He−Ne laser light scattering apparatus and the methodology used for the detection of phase transitions have very recently been described in great detail.[9] The cell (internal volume ∼1.0 cm^3, optical length ∼2.6 mm) is a thick-walled Pyrex glass tube connected to a pressurization line and separated from it by a mercury plug. Scattered light intensity is captured at a very low angle (2 < $2\theta/$deg < 4) in the outer part of a bifurcated optical cable,[14] while transmitted light is captured in the inner portion of this cable. Scattered (I_{sc}) and transmitted light (I_{tr}) are corrected for density fluctuations, reflections, and multiple scattering effects[15] according to Debye's theory. The cloud point is the point on the $1/I_{sc,corr}$ against pressure (P) or temperature (T) least-squares fits where the slope changes abruptly. The operational spinodal point will be taken at the interception point where $1/I_{sc,corr} = 0$. At this point, the intensity of scattered light has an infinite value. A comprehensive discussion of the methodology of these calculations can be found elsewhere.[14] Cloud-point temperature accuracy is typically ±0.01 K in the range 240 < T/K < 400, decreasing to ±1 K in the case of spinodals, which are obtained from a large extrapolation to the point where the inverse of the scattered light intensity reaches a null value. As for pressure, accuracy is ±0.1 bar up to 50 bar. This value is the upper limit of pressure for the glass capillary cell.

In the case of experiments where pressure was raised above 50 bar (and up to 700 bar), a novel sapphire/stainless steel cell replaced the original glass capillary one. The cell is schematically represented in Figure 2. In this case, the hydraulic fluid is the pure solvent (in this work, water) in
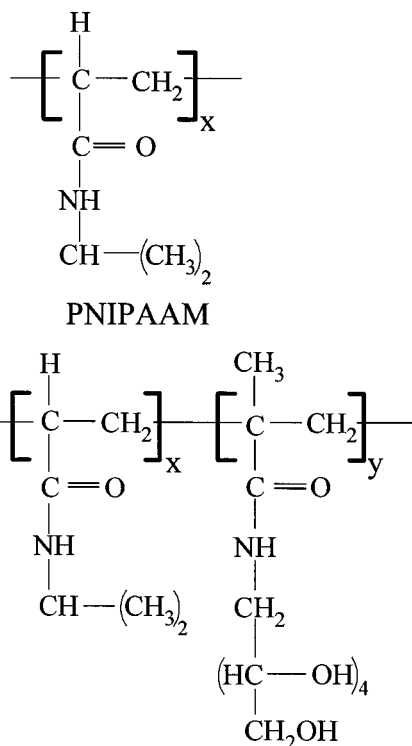

Figure 1. Scheme of the molecular structures of the repeating units in PNIPAAM and in copoly(PNIPAAM$_x$/VS$_y$) where on average $x/y \approx 6.5$ (see text).
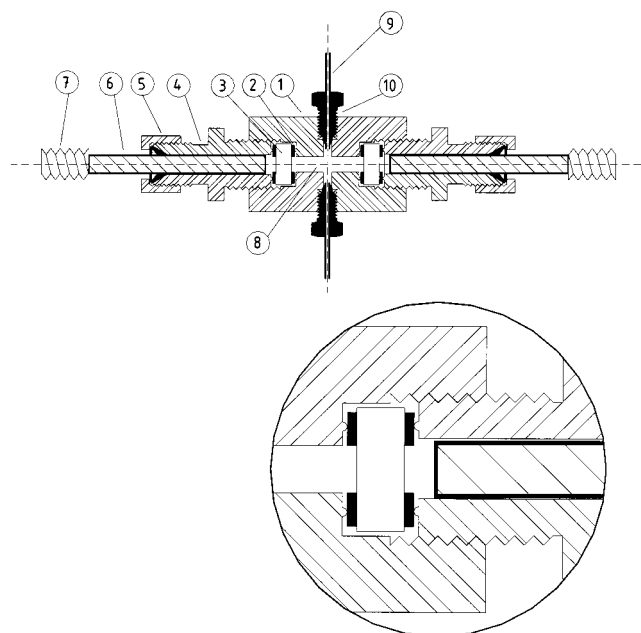
Figure 2. High-pressure stainless steel (SS) sapphire cell: 1, SS cell's body; 2, copper gasket; 3, sapphire window (o.d. = 0.5 in. (12.7 mm) and thickness = 0.125 in. (3.175 mm); 4, SS male connector; 5, $^{1}/_{4}$ in. SS nut; 6, $^{1}/_{4}$ in. SS rod acting as a shield for the optical fibers which are located inside; 7, flexible SS hose; 8, sample within the optical volume of ∼0.5 cm³; 9, 1/16 in. SS tubing; 10, AF1-type fitting. The inset shows an enlargement of how the sealing on both polished surfaces of the sapphire windows is made.

contact with a sufficiently long (1/16 in.) SS tube filled with the solution (buffer volume),[16] in order to avoid contamination during compression/expansion cycles. This possible contamination of the sample under study by the hydraulic fluid was judged by mixing dye in the latter. The optical volume inside the cell never showed any traces of the dye after several cycles of pressurization. The total volume (buffer + optical) of injection of solution is typically 1.6 cm³, although the optical volume roughly corresponds to a mere 0.5 cm³. In this newly designed sapphire-windowed cell, the optical path length is about 8 times longer (∼20 mm) than that in the glass capillary one. Consequently, the detection of phase transitions becomes sharper and permits the study of solutions that present low level of turbidity upon phase separation, such as the current ones. Nonetheless, the low-angle scattered signal is lost. Typical runs (isobaric and isothermal) showing the sharp decrease of transmitted light as phase separation occurs are plotted in Figure 3. Therefore, cloud points are accurately determined as the point where a kink in the transmitted signal is observed, but no operational spinodal can be detected. In the case of isothermal runs, cloud-point temperature accuracy was maintained (±0.01 K), but it worsens to ±0.1 K for isobaric runs. As for pressure, the uncertainty is ±1 bar in this higher pressure range.

Solutions were made up gravimetrically and left stirring for several hours (sometimes for several days) in sealed vials before being injected into the measuring cell.

3. Results and Discussion

In this work, we studied seven polymeric systems (see Table 1) in H_2O. The set of all copolymers has an average ratio in the number (x) of isopropylacrylamide attached labels to that of VS (y) of $x/y = 6.5 \pm 0.2$. In other words, within the limits of sufficient precision the copolymers differ from each other merely in respect to their respective molecular weight. In a previous preliminary work[8] we checked that the composition dependence of the phase diagrams of one PNIPAAM sample
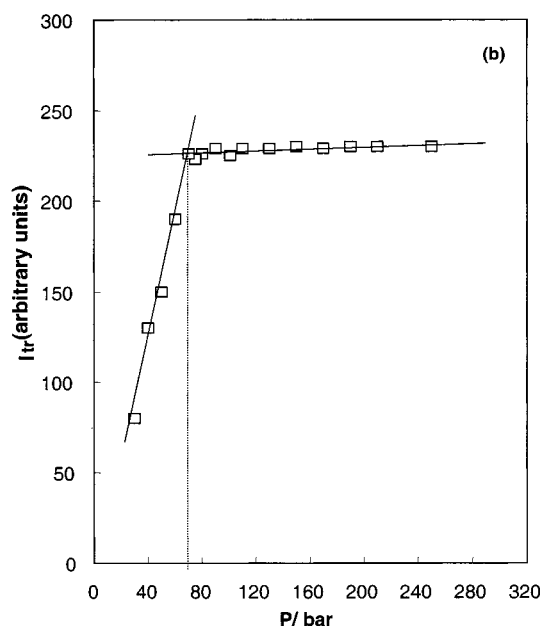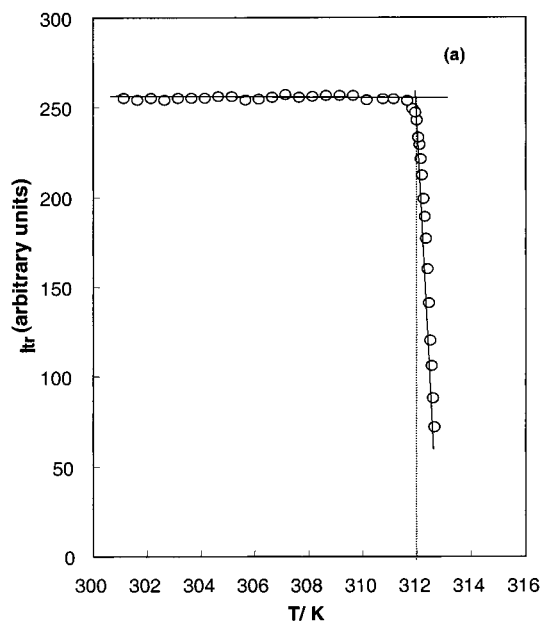

Figure 3. Examples of isobaric (a) and isothermal (b) runs during phase transition plotted as transmitted intensity vs T or p, respectively. The dashed lines locate the cloud-point temperature or pressure. (a) P3 (3.07 wt %) + water solution at $p = 262.5$ bar run; (b) CP1 (4.32 wt %) + water solution at $T = 310.3$ K run.

as well as of the higher molecular weight CPs is quite uninteresting—(T, x) phase diagrams are pretty flat. The exception to this rule lies either in the highly diluted polymer region (<1 wt %) or in the case of CPs of very low MW.

In the current work we therefore focused our attention mainly on the pressure dependence of the equilibria involved at or near-critical composition and checked simply 2−3 isopleths. Only in the case of the low MW copolymer, CP4, composition effects were also analyzed in some detail to test our previous hypothesis[8] that we were approaching the neighborhood of a hypercritical region.

Gomes de Azevedo et al.[8] showed that critical concentrations for this type of systems are about 6 wt % in polymer, decreasing slightly to lower values as pressure
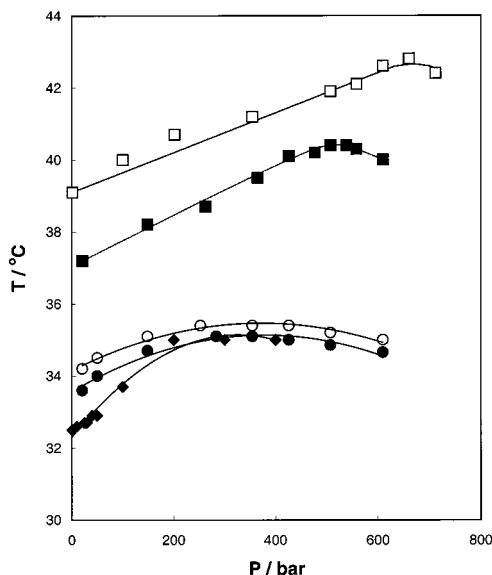
Figure 4. Experimental (T–p) isopleths of cloud points of several PNIPAMs in water: diamonds (P1), circles (P2), and squares (P3). See Table 1. Black is for near-critical isopleths (4.00, 2.95, and 3.07 wt %), while white is for off-critical (diluted) ones (between 0.35 and 0.39 wt %). Lines were drawn as guides for the eye.

is increased. Within the pressure range used in this work (1–700 bar), the average critical composition is estimated to be of the order of 5 ± 1 wt %. Although critical concentration is not accurately known, conclusions inferred from the current results are not affected by this fact. For any given system, we have checked that the T–p behavior of phase transitions is very similar within a broad range of polymer concentrations (0.3–5.5 wt %). This is in agreement with previous observations using other polymeric solutions.[9,14,17] All T–p isopleths investigated can thus be considered at critical or near-critical concentration. The whole set of (T, p, wt %) data for all seven aqueous solutions of polymer samples (Table 1) is reported as Supporting Information.

A. System (PNIPAAM + H_2O). Figure 4 illustrates the pressure dependence of the transition temperature for three molecular weights at distinct compositions. In agreement with other authors,[1,3,6] we have also witnessed the almost negligible MW dependence of the phase diagram of PNIPAAM within a ca. 4 K interval for similar isopleths. Nevertheless, the accuracy of the present results along with the comparable polydispersities of the distinct samples (Table 1) permits us to establish that, rigorously speaking, T increases as MW decreases (and even more markedly for low MWs), as should be expected for a LCST-type transition. It can also be observed that concentration effects are subtle.

As for pressure, although it also has a weak effect on the temperature of the transition, T–p behavior is quite interesting, presenting maxima and, thus, change in the sign of the slope. The location of these maxima matches relatively well with those already reported by Otake et al.[6] This change in sign could be accounted for by a corresponding change in sign of the excess volume, v^E, from negative to positive as pressure is raised.[13,18] Therefore, while pressure initially favors mixing, the opposite occurs for high pressures. In between these two distinct trends, ideal mixing ($v^E = 0$) should incidentally occur. The location of the maximum seems to shift to increasingly higher pressures as M_w decreases. In other words, it should be noted that this behavior constitutes

an indication that some isothermal (p, wt %) cuts of the phase diagram present both an upper critical solution pressure (UCSP) and a lower critical solution pressure (LCSP). This type of phase diagram will evolve to an "hourglass" one (in the (p, wt %) representation) by temperature increase[13] as the upper and lower branches merge (the maximum in the T–p isopleths). The region where this change occurs has been called the hypercritical region.[13,17,18] In it, both the near-critical isopleths and the critical one present (dp/dT) = ∞ at a given point. For the latter, the point is a singular one where two critical loci (the locus of critical points of the UCSP branch and that of the LCSP) merge. It is represented as a dot joining the two branches in the (p, wt %) diagram of a binary mixture. Thus, it is a double critical point, more specifically, a pressure–double critical point (p–DCP) as opposed to other situations where the singular point is seen in the (T, wt %) diagram (temperature–double critical point (T–DCP); see next subsection).[19] The term double critical point (and critical double point) has been widely used for these situations (see the review paper of Narayanan and Kumar[21] and references therein) and the meaning of "double" is twofold: (i) two critical loci join at a point, and (ii) the divergences to infinity of response functions to criticality such as osmotic compressibility and correlation length are expected to double their exponents at these extrema of T–p (or p–T) critical lines.

B. System [Copoly(PNIPAAM/VS) + H_2O]. Most of the copolymers of PNIPAAM studied so far have been of the hydrophobically modified type.[1] Aqueous solutions of these copolymers present lower LCST temperatures than those of PNIPAAM. A similar effect is obtained when a hydrophilic compound is added to the solution[4,8] (competition between the compound and the polymer for dissolution), but the opposite should be observed (rise of the LCS temperature) if that compound is incorporated in the polymer backbone. This is the case for the CPs investigated in the current work (Table 1), where a vinylsaccharide label was attached to the chain. A sample of the most relevant results of cloud points appears in Figure 5.

The immediate striking feature is the observance of a drastic phase behavior for the low-MW copolymer (CP4). In the case of the high-MW copolymers, all phase behavior basically resembles that of PNIPAAM; i.e, it demonstrates subtle MW and pressure dependence (($\partial T/\partial p)_{\lim P \to 0} \approx 4 \times 10^{-3}$ K bar^{-1}) of the temperature of transition. Also, the composition effects are relatively modest. They represent a pressure-independent increase of 2 K for CP1 in going from 4.3 to 0.38 wt % and of 5 K for CP3 from 4.0 to 0.70 wt % (see Supporting Information). In contrast, CP4 shows ($\partial T/\partial p)_{\lim P \to 0} \approx 15$ K bar^{-1}, corresponding to an increase of 3 orders of magnitude. Both the enhanced pressure and composition effects for this low-MW CP can be appreciated in Figure 6. These facts, along with the observation that the MW dependence is also extremely enhanced in this low-MW region, constitute fingerprints of the vicinity of a temperature hypercritical region with its T-DCP ($\partial T/\partial p = \infty$, $dp^2/dT^2 < 0$). Were it possible to experimentally work at temperatures above 470 K, one could observe reentrant T–p isopleths at high temperature (maxima in p–T plots). Here, it is the enthalpic behavior that suffers a change from exothermal (LCST) to endothermal (UCST) as temperature increases. Above a certain (low) pressure
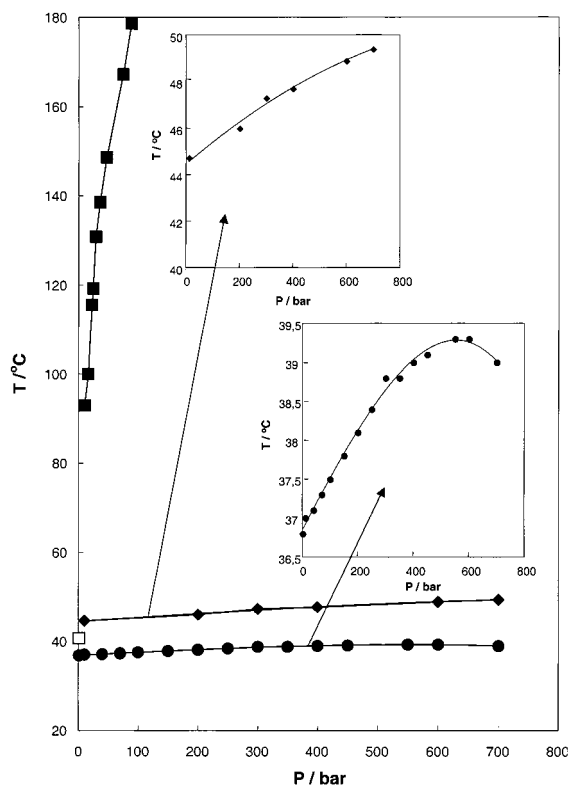
Figure 5. Experimental ($T-p$) near-critical isopleths of cloud points of several copolymers in water: (●) CP1 ($M_w = 432\,000$, 4.3 wt %); (□) CP2 ($M_w = 170\,000$, 3.01 wt %); (◆) CP3 ($M_w = 110\,000$, 2.3 wt %); (■) CP4 ($M_w = 56\,000$, 5.5 wt %). It should be noted that for CP4 solutions all actual values of pressure were in the plot multiplied by a factor of 10. Full lines are guides for the eye. Insets are enlargements to show the details of the $T-p$ isopleths of CP1 and CP3.
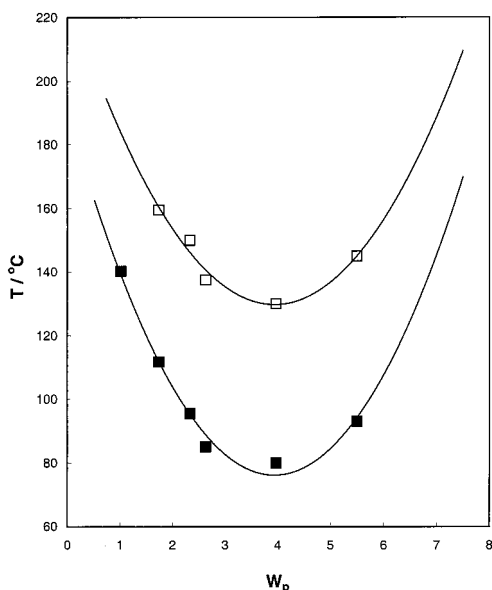

Figure 6. Exceptionally strong pressure and composition dependence of the phase diagram of CP4 + water. Wp = copolymer wt %. (■) = 1 bar; (□) = 3 bar.

this aqueous solution of CP₄ is always homogeneous (one phase).

In summary, these copolymers represent a single system that changes from pressure hypercritical behavior to a temperature hypercritical one just by decreasing the chain length. At low temperature, high MW, and high pressure, the volumetric properties are expected

to change, while in the region of high temperature, low MW, and low pressure, one should predict changes in the enthalpic properties. The system changes smoothly from one extreme to the other. This is well exemplified by CP₃ (see insets to Figure 5), corresponding to an intermediate $T-p$ trend between those of CP₁ and CP₄.

C. Modeling. Recently, de Sousa and Rebelo[10] presented in great detail a robust algorithm for a modified Flory–Huggins model, which considers a concentration- and temperature-dependent[11,12] interaction parameter, χ. The Gibbs energy of mixing per mole of segment unit is given by

$$\frac{\Delta G_m}{RT} = \frac{\phi_A}{r_A} \ln \phi_A + \frac{\phi_B}{r_B} \ln \phi_B + \phi_B \int_{\phi_B}^{1} \chi(\phi, T)\, d\phi \quad (1)$$

where the ϕ_i's are the segment fractions and r_i's the segment numbers, with the subscripts A and B meaning solvent and polymer, respectively. χ is the reduced excess interaction energy assumed to be given by

$$\chi(\phi_B, T) = B(\phi_B)\, D(T) = \left(\sum_{i=0}^{n} b_i \phi_B^i\right)\left(d_0 + \frac{d_1}{T} + d_2 \ln T\right) \quad (2)$$

where b_i's and d_i's are constants for respectively the composition and temperature dependence of the excess energy.

A straightforward thermodynamic manipulation shows that the underlying excess enthalpy per mole of segment unit for this model is given by

$$\frac{H_m^E}{RT} = \left(\frac{d_1}{T} - d_2\right)\phi_B \int_{\phi_B}^{1} B(\phi_B)\, d\phi \quad (3)$$

If one seeks to estimate the excess volume taken from the model's result, the algorithm has to be extended in order to accommodate pressure effects. Rebelo[13] showed that the simplest g^E model compatible with all known basic types of L–L phase diagrams is one in which the excess enthalpy is linear in T (such as in eq 3) but quadratic in p. The set of equations for the pressure dependence (d_2 continues pressure independent) of the parameters is now

$$d_0(p) = \frac{1}{R}(C + B_1 p); \quad d_1(p) = \frac{1}{R}(A_0 + A_1 p + A_2 p^2) \quad (4)$$

where C, B_1, and A_i's are parameters with physical meaning.[13] Thus, for the excess volume

$$V_m^E = (A_1 + 2A_2 p + B_1 T)\phi_B \int_{\phi_B}^{1} B(\phi_B)\, d\phi \quad (5)$$

and for the excess isobaric heat capacity

$$C_p^E = -d_2 R \phi_B \int_{\phi_B}^{1} B(\phi,)\, d\phi \quad (6)$$

Table 2 reports the model's fitted parameters to 16 (T, ϕ, $p = 1$ bar) experimental points of aqueous solutions of PNIPAAM (P1), and Figure 7 shows the modeled cloud-point curve and the spinodal one. The algorithm was used in its monodisperse version at fixed M_n. Calculations using its polydisperse version are currently in progress. Since we are dealing with ratios of $M_w/M_n \sim 2$, most likely polydispersity effects are

Table 2. Monodisperse Modeling Parameters and Results (See Eqs 1 and 2) for Sample P1 Aqueous Solutions of PNIPAAM[a]

M_w	615000	d_1	−6783.8274
M_n	301471	d_2	−14.392121
b_0	1.000000	M_s	113.00
b_1	0.857399	n	2667.9
b_2	0.0650176	ϕ_c	0.1305
b_3	0.000000	T_c(UCST)/K	779.1
b_4	0.000000	T_c(LCST)/K	306.4
d_0	105.03495		

[a] n is the number of monomers of a number-averaged copolymer chain. ϕ_c is the critical segment fraction of copolymer.
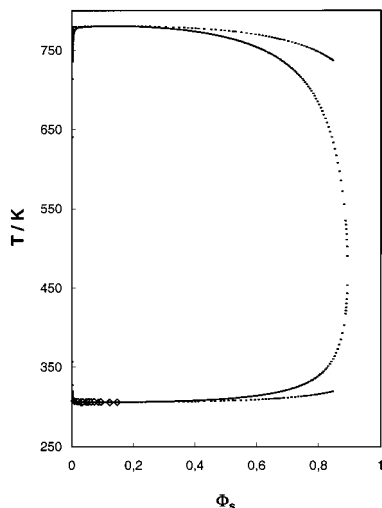

Figure 7. Modeled results (monodisperse version) obtained by fitting to the experimental points (open diamonds) of aqueous solutions of P1 ($M_w = 615\,000$) at $p = 1$ bar. ϕ_s represents the polymer segment fraction. The two-phase region is inside the envelope. Outer curve stands for the binodal points, and inner curve shows the spinodal ones.

Figure 8. Modeled results (see eq 3 and Table 2) for the excess enthalpy, h^E, in J mol^{-1} segment^{-1} vs polymer segment fraction, Φ_s, of (P1 + water) at $p = 1$ bar. Results are represented for eight temperatures. While at 300 K (or below) and at 800 K (or above) the (P1 + water) system is in its one-phase region irrespective of concentration; at all other intermediate temperatures there is some window of immiscibility. The straight lines in the h^E vs Φ_s plot represent the two-phase region.

large. A detailed discussion comparing polydisperse and monodisperse cases at fixed M_n or fixed M_w can be found elsewhere.[10] The authors concluded that it is more theoretically sound to use the fixed M_n approach. Computed results yield for the enthalpic effect upon mixing at 300 K (measured as the precomposition factor in eq 3 multiplied by RT) the value −20.5 kJ mol^{-1} segment^{-1}, which is of the same order of magnitude as the hydrogen-bond interaction.[22] The behavior of the excess enthalpy of PNIPAAM's aqueous solutions versus temperature and composition is plotted in Figure 8. At 300 K, the computed equimolar segment enthalpy of mixing is −8.7 kJ mol^{-1} segment^{-1}. This exothermic value conforms to the reported[3,5] endothermic enthalpies of phase transition near 300 K using differential scanning calorimetry, $\Delta H_t = +5.8 \pm 1$ kJ mol^{-1} monomer^{-1}. It should be noted that the difference between the quantities H^E and ΔH_t should not merely correspond to the symmetry of their signs. Their relative values should be distinct, for demixing does not lead to the pure components state and one monomer unit corresponds to ca. five segments. The plot in Figure 8 at 306.53 K is illustrative. Demixing leads to the equilibrium between an almost pure water phase and a "rich" polymer one of segment fraction ca. 0.4. In other words, $|H^E| > |\Delta H_t|$. As for C_p^E, the precomposition factor in eq 6 is +120 J mol^{-1} segment^{-1} K^{-1}. The theoretical results (Figure 7) show that phase separation is more of the precipitation type (one of the phases is basically the pure component) than of the typical L−L partial miscibility type. This is
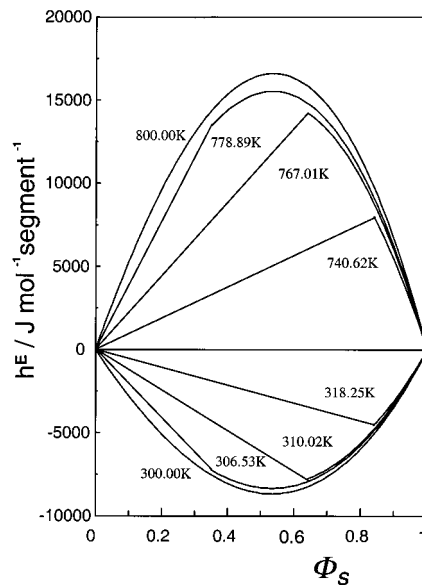
in good agreement with the experimental observations. Both LCST and UCST branches are fairly flat with the latter occurring at too high a temperature to be experimentally accessible (T_c(LCST) = 306. 5 K; T_c(UCST) = 779.1 K).

In regards to copolymer aqueous solutions, Table 3 reports the model's fitted parameters to experimental points obtained at a nominal pressure of 1 bar. Figure 9 shows the modeled cloud-point curves. For sake of clarity, spinodal lines have not been included in the plot. Computed results yield for the enthalpic effect upon mixing at 300 K the value −2.81 ± 0.01 kJ mol^{-1} segment^{-1}, irrespective of the polymer chain length. This value is 1 order of magnitude smaller than that found for PNIPAAM, a fact which can account for the possibility of formation of multiple intramolecular hydrogen bonds that are competing with the intermolecular ones. As for C_p^E, the precomposition factor in eq 6 goes, irrespective of temperature, smoothly from +17.8 to +19.3 J mol^{-1} segment^{-1} K^{-1} as one moves from CP1 to CP4.

Figure 9 nicely illustrates the speed at which the experiments approach the vicinity of temperature−hypercritical conditions as one moves toward the CP4 phase diagram region. The (T, ϕ) closed-loop diagram is markedly shrunk here. Any small increase in pressure or decrease in MW will make this closed-loop envelope to evolve to a single dot (T−DCP). This should occur at a temperature that can be estimated by the condition $(\partial T/\partial \phi) = \infty$, $T \cong 445$ K. This value compares favorably with a preliminary reported[8] rough estimation of 430 K. Those authors[8] used the T vs (MW$^{-1/2}$) Imre−Van Hook representation[23] to locate that point. The original scaling relation of Imre and Van Hook corresponds to a symmetrical expansion around an assumed hypercritical point in the T−MW$^{-1/2}$ plane. Both the experimental and computed values of phase separation for the co-

Table 3. Monodisperse Modeling Parameters and Results (See Eqs 1 and 2) for All Aqueous Solutions of Copolymers[a]

	CP1	CP2	CP3	CP4
M_w	432000	170000	110000	56000
M_n	145455	77982	51643	28571
VS cont (mol %)	14.0	12.9	13.7	13.3
b_0	1.000000	1.000000	1.000000	1.000000
b_1	1.35938556	1.2951954757	0.47681173493	−1.6702232133
b_2	−1.1694941407	−1.2605451763	−1.2741398126	−1.2845054102
b_3	0.000000	0.000000	0.000000	0.000000
b_4	0.000000	0.000000	0.000000	0.000000
d_0	15.945587086	16.686205876	16.972896602	17.207098273
d_1	−981.53071497	−1013.5068607	−1025.26810	−1035.9101566
d_2	−2.1440329013	−2.2558208692	−2.2916102178	−2.3254142523
M_s	132.04	130.544	131.632	131.088
n	1101.598	597.362	392.329	217.953
ϕ_c	0.1399	0.1315	0.060	0.032
$T_c(UCST)/K$	724.2	682.5	665.9	561.0
$T_c(LCST)/K$	307.5	311.3	314.9	359.6

[a] n is the number of monomers of a number-averaged copolymer chain. ϕ_c is the critical segment fraction of copolymer.
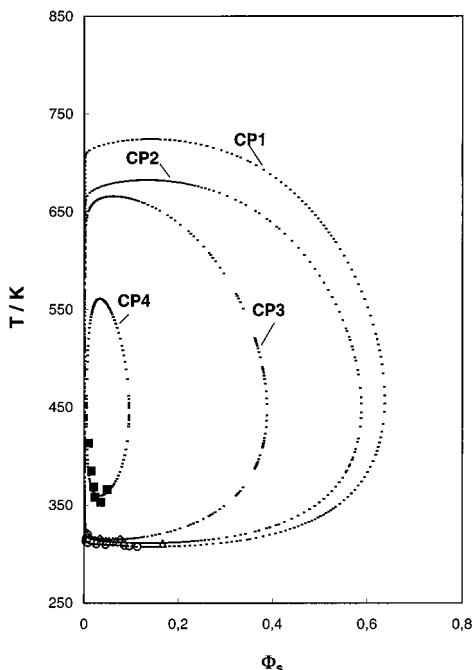

Figure 9. Temperature−composition (copolymer segment fraction) phase behavior of all copolymers aqueous solutions at 1 bar: large symbols, experimental points; dotted lines, modeled binodals. Spinodal curves are not shown for sake of clarity.

Figure 10. Critical temperature of transition vs $(M_n)^{-1/2}$ for all copolymers at 1 bar: (×) from experimental data; (○) from modeling (see Table 3).

polymers in this plane (now rephrased as T vs $M_n^{-1/2}$ plot) are represented in Figure 10. The plot is clearly nonsymmetrical with the hypercritical point shifting toward the LCST branch. Therefore, we adopted the following modified version of the Imre−Van Hook relation:

$$\left|\frac{T_c - T_c^*}{T_c^*}\right|^b = A\left|\frac{X - X^*}{X^*}\right|^\alpha \tag{7}$$

where $X = M_n^{-1/2}$ and the superscript * refers to conditions which locate the hypercritical point. In the case of the LCST branch $b = 1$, but in the UCST one $b = 0.365$ to account for its larger amplitude. The full line in Figure 10 was generated from an expansion around the point ($T_c^* = 413$ K, $X^* = 0.006$). All three estimations (see above) of the hypercritical temperature at a nominal pressure of $p = 1$ bar are in reasonably good agreement.
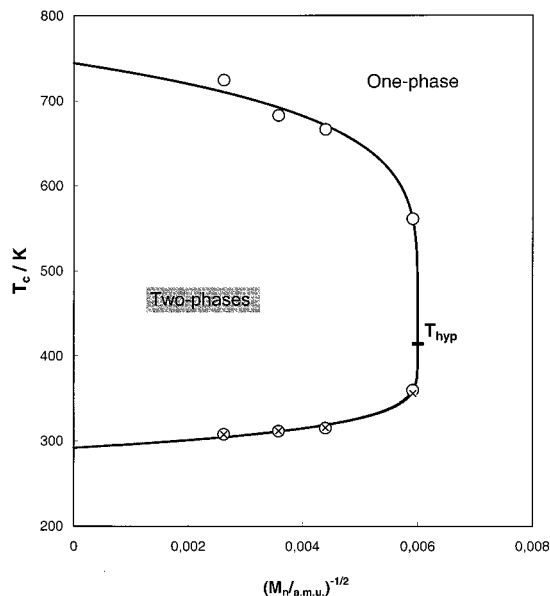
It has been shown (refs 13, 18, and references therein) that the slope of the $T−p$ critical loci is intimately related to the second derivative in respect to composition of the mixture's volume and enthalpy through

$$\left(\frac{\mathrm{d}T}{\mathrm{d}p}\right)_c = \lim_{\substack{T \to T_c \\ x \to x_c}} \frac{\partial^2 v_M/\partial x^2}{\partial^2 s_M/\partial x^2} = \lim_{\substack{T \to T_c \\ x \to x_c}} T\frac{\partial^2 v_M/\partial x^2}{\partial^2 h_M/\partial x^2} \tag{8}$$

It is also well-known that, in order for a LCST to occur, it is necessary that

$$\left(\frac{\partial^2 h_M}{\partial x^2}\right)_c = \left(\frac{\partial^2 \Delta h_{mix}}{\partial x^2}\right)_c = \left(\frac{\partial^2 h^E}{\partial x^2}\right)_c > 0 \tag{9}$$

whereas for an UCST, the above inequality is of opposite sign. Therefore, the sign of $(\mathrm{d}T/\mathrm{d}p)_c$ establishes that of the second derivative of the molar volume of the mixture in respect to composition. Although it entails some loss of generality, it is much more interesting to relate the slope of the critical loci to the excess functions themselves rather than to their second derivatives. If the distinct excess functions strictly conform to each other

in respect to their composition dependence, then, independent of the presence of anomalies such as inflection points, the following relation

$$\left(\frac{dT}{dp}\right)_c \approx \frac{T_c v_c^E}{h_c^E} \approx \frac{T_c A_{(v^E)}}{A_{(h^E)}} \tag{10}$$

should be also verified. In eq 10, $A(v^E)$ and $A(h^E)$ represent the precomposition factors of the excess volume and excess enthalpy, respectively. The above-mentioned simplification (the second approximate equality in eq 10) is valid if the excess Gibbs energy of mixing does not present cross temperature− or pressure−composition terms. The currently adopted model (see eqs 1−5) conforms to this. Therefore, for instance, a T−DCP and a hypercritical region occur at T where $h^E = 0$. Using the model's terminology, $T_{hyp} = d_1/d_2$, which results in $T_{hyp} = 445.5$ K for CP4 aqueous solution at $p = 0.1$ MPa.

An estimation of the volume effects upon mixing can be assessed using eq 10 and by combining the experimentally accessible values of $(dT/dp)_c$ with the computed ones for $A(h^E) = R(d_1 − d_2 T_c)$ at 0.1 MPa. Taking into account the fact that the experimental functional composition dependence of the excess functions is unknown and that, in this study, the systems are being modeled as monodisperse, the results should be interpreted with some care. Although the actual numerical values of $A(v^E)$ cannot be taken too strictly due to the simplifications involved, the observed trends in their magnitude as one moves from P1 to the copolymers and within the copolymers is very informative. In the case of P1 we obtained $A(v^E) = −3.2$ cm³ mol⁻¹ segment⁻¹, a value which corresponds approximately to a 10-fold effect when compared to that found for both CP1 and CP3 but a 100 times smaller effect than that estimated for CP4. The excess volumes themselves are smaller than these precomposition factors since polymer segment fractions do not typically exceed $\phi_p = 0.1$.

With the above-mentioned caveats in mind, it is interesting to note that these excess volumes conform reasonably well to the experimental ones available in the literature.[6] These authors report a volume increase due to the aggregation of polymer chains upon demixing at atmospheric pressure of $(10.6/5) \sim 2$ cm³ mol⁻¹ segment⁻¹. Unfortunately, there are no volumetric data available for the copolymers.

The theoretical framework described by eq 10 is a very useful one, for it can predict exceptionally interesting phase behavior[24] including the potentially possible demixing phenomena in racemic mixtures at high pressure[25] due to positive, albeit very small, excess volumes exhibited by enantiomers.

The importance of the relations established by eqs 8−10 has just been proven. Nevertheless, one should be cautious about their blind application. Some systems may not fulfill the approximations involved,[26] which can lead to misleading conclusions.

Imre et al.[26] performed a sound set of experiments in order to establish a relationship between the ratio of lengths of polymer and/or oligomer chains and the location of a possible p−DCP (of the UCST branch) for weakly interacting chemical species. The general conclusion is that, while for polymer blends (thus large size−large size systems, but with components of "similar" size) one finds that the golden rule is $(dT/dp) > 0$ ($v^E > 0$), commonly, in polymer solutions (large size−

small size systems) $(dT/dp) < 0$ ($v^E < 0$), which may evolve to a change of sign at high pressures. Similar trends have been observed for long-chain oligomers + small chain oligomers. Those authors discuss this behavior in terms of the location of the $(T−p)$ minimum, which locates the p−DCP. And they conclude that, most probably, for those systems where $(dT/dp) > 0$ at atmospheric pressure, there is a pressure−hypercritical region lying in the "hidden" mechanically metastable domain[27,28] of $p < 0$. We do agree with this phenomenological analysis and would like to further point out that molecular fluid mixtures (small size−small size systems, but "similar" sizes of the components) usually also show[29−31] $(dT/dp) > 0$ for the UCST. Using a simple molecular approach, one can state that when the components are of similar size (whether they be large or small) there is a natural tendency for them to mix by expansion, while, when the sizes are too different, they tend to contract upon mixing. Thus, for weakly interacting systems of similar sizes and for $h^E > 0$ (hetero attraction weaker than the homo attraction) at the UCST one should expect a commensurate (both in sign and in value) v^E, reflecting some incompatibility among the mixture's components. Thus, $v^E > 0$ and $(dT/dp) > 0$. In cases where the components are very distinct in size, there is significant free volume to accommodate the smaller component within the interspersed space left by the larger one. The mixing process can thus evolve through compression. Thus, $(dT/dp) < 0$ ($v^E < 0$). At high pressures (high densities) there is no more room for compression upon mixing, and all binary systems irrespective of their ratio of sizes should show $(dT/dp) > 0$ ($v^E > 0$). Therefore, at intermediate pressures one should be able to locate a pressure−hypercritical region. This hypercritical region will usually be found at "expanded states" (absolute negative pressures[27,28]) for similar-size systems, as the higher compressibility that allows compression has been restored by mechanically pulling the molecules apart.

In LCST-type of demixing the above-discussed simple molecular explanation becomes more complicated by virtue of the more complex nature of LCST phase transitions. Typically, LCST occurs at high temperatures (above UCST) for weakly interacting systems due to the proximity of the critical point of one of the components. This component is highly expanded in its pure state and suffers a large compression upon mixing ($v^E < 0$). Nonetheless, here $(dT/dp) > 0$ because $h^E < 0$. The other common type of LCST (the low-temperature one below an UCST) occurs in strongly oriented-like interactions such as those induced by hydrogen bonding. This type of behavior is found when one or both of the pure components exhibits self-association due to H-bonding, while chemically complex strong intercomponent HB can also occur in the mixture. There is again a release of energy upon mixing ($h^E < 0$), but the sign of v^E is very difficult to predict a priori.[29,32] This leads to the exceptionally rich behavior observed[32] even for small-components solutions.

In the cases under study in the current work, we conclude that (i) at low pressure all systems should experience a contraction upon mixing and (ii) the contraction in PNIPAAM is greater than that in the high-MW CPs because, while in the first case, one expects the influence of intermolecular H-bonds; in the latter, there is competition between inter- and intramolecular H-bonds, which dampens the effect. In any case,

H-bonding seems to be the key factor responsible for the release of energy upon mixing.[3] In contrast, the contraction upon mixing at low densities seems to be governed by virtue of the hydrophobic interaction.[6] As density increases though, the HB effect (which can sometimes contribute to an expansion upon its formation) overwhelms the hydrophobic interaction effect (which should contribute to compression upon mixing) and, thus, the excess volume becomes positive.

At low pressures, the high-temperature, low-MW CP4 system shows exceptional thermodynamic properties with h^E low and changing sign and a predicted unusually high negative value for v^E. This behavior translates as a strong expansion upon phase separation. This phenomenon was actually experimentally observed while performing isobaric runs in CP4 solutions for the detection of phase separation. We observed strong increases (sometimes of 100%) of pressure when one-phase/two-phase transitions occurred. We have never witnessed anything similar in any other systems previously studied.[9,14,17,33−35]

Supporting Information Available: Table of cloud-point temperatures, T_{cp}, and pressures, P, at distinct polymer weight percent, W_p, of aqueous solutions of polymer samples. This material is available free of charge via the Internet at http://pubs.acs.org.

References and Notes

(1) Shild, H. G. *Prog. Polym. Sci.* **1992**, *17*, 163−249.
(2) Shild, H. G.; Muthukumar, M.; Tirrel, D. A. *Macromolecules* **1991**, *24*, 948−952.
(3) Shild, H. G.; Tirrel, D. A. *J. Phys. Chem.* **1990**, *94*, 4352−4356.
(4) Kim, Y.-H.; Kwon, I. C.; Bae, Y. H.; Kim, S. W. *Macromolecules* **1995**, *28*, 939−944.
(5) Fujishige, S.; Kubota, K.; Ando, I. *J. Phys. Chem.* **1989**, *93*, 3311−3313.
(6) Otake, K.; Karaki, R.; Ebina, T.; Yokoyama, C.; Takahashi, S. *Macromolecules* **1993**, *26*, 2194−2197.
(7) Klein, J.; Herzog, D. *Makromol. Chem.* **1987**, *188*, 1217−1232.
(8) Gomes de Azevedo, R.; Rebelo, L. P. N.; Ramos, A. M.; Szydlowski, J.; de Sousa, H. C.; Klein, J. *Fluid Phase Equilib.* **2001**, *185*, 189−198.
(9) de Sousa, H. C.; Rebelo, L. P. N. *J. Chem. Thermodyn.* **2000**, *32*, 355−387.
(10) de Sousa, H. C.; Rebelo, L. P. N. *J. Polym. Sci., Polym. Phys.* **2000**, *38*, 632−651.
(11) Qian, C.; Mumby, S. J.; Eichinger, B. E. *Macromolecules* **1991**, *24*, 1655−1661.
(12) Mumby, S. J.; Sher, P. *Macromolecules* **1994**, *27*, 689−694.
(13) Rebelo, L. P. N. *Phys. Chem. Chem. Phys.* **1999**, *1*, 4277−4286.
(14) Szydlowski, J.; Rebelo, L. P. N.; Van Hook, W. A. *Rev. Sci. Instrum.* **1992**, *63*, 1717−1725.
(15) Kiepen, F.; Borchard, W. *Macromolecules* **1988**, *21*, 1784−1790.
(16) Van Hook, W. A.; Wilczura, H.; Rebelo, L. P. N. *Macromolecules* **1999**, *32*, 7299−7311.
(17) Luszczyk, M.; Rebelo, L. P. N.; Van Hook, W. A. *Macromolecules* **1995**, *28*, 745−767.
(18) Schneider, G. M. *Ber. Bunsen-Ges. Phys. Chem.* **1966**, *70*, 497−520.
(19) It should be noted that a recently published article by Bolz et al.[20] contains the IUPAC recommendations for the nomenclature of phase diagrams. According to them, in a (T, x)-type closed-loop, the p-DCP is called an *hyperbolic* (in p−x) *maximum temperature critical point* and the T-DCP is called an *elliptic* (in T−x) *maximum pressure critical point.*
(20) Bolz, A.; Deiters, U. K.; Peters, C. J.; de Loos, T. W. *Pure Appl. Chem.* **1998**, *70*, 2233−2257.
(21) Narayanan, T.; Kumar, A. *Phys. Rep.* **1994**, *249*, 135−218.
(22) Rozenberg, M.; Loewenschuss, A.; Marcus, Y. *Phys. Chem. Chem. Phys.* **2000**, *2*, 2699−2702.
(23) Imre, A.; Van Hook, W. A. *J. Phys. Chem. Ref. Data* **1996**, *25*, 637−661.
(24) Schneider, G. M.; Scheidgen, A. L.; Klante, D. *Ind. Eng. Chem. Res.* **2000**, *39*, 4476−4480.
(25) Kenney, J. F.; Deiters, U. K. *Phys. Chem. Chem. Phys.* **2000**, *2*, 3163−3174.
(26) Imre, A.; Melnichenko, G.; Van Hook, W. A.; Wolf, B. A. *Phys. Chem. Chem. Phys.* **2001**, *3*, 1063−1066.
(27) Imre, A.; Martinás, K.; Rebelo, L. P. N. *J. Non-Equilib. Thermodyn.* **1998**, *23*, 351−375.
(28) Imre, A.; Van Hook, W. A. *Chem. Soc. Rev.* **1998**, *27*, 117−123.
(29) Rowlinson, J. S.; Swinton, F. L. *Liquids and Liquids Mixtures*, 3rd ed.; Butterworth: Kent, 1982.
(30) Prausnitz, J. M.; Lichtenthaler, R. N.; Azevedo, E. G. *Molecular Thermodynamics of Fluid Phase Equilibria*, 2nd ed.; Prentice Hall Inc.: Englewood Cliffs, NJ, 1986.
(31) Myers, D. B.; Smith, R. A.; Katz, J.; Scott, R. L. *J. Phys. Chem.* **1966**, *70*, 3341−3343.
(32) Schneider, G. M. *Ber. Bunsen-Ges. Phys. Chem.* **1972**, *76*, 325−331.
(33) Rebelo, L. P. N.; Van Hook, W. A. *J. Polym. Sci., Polym. Phys.* **1993**, *31*, 895−897.
(34) Rebelo, L. P. N.; de Sousa, H. C.; Van Hook, W. A. *J. Polym. Sci., Polym. Phys.* **1997**, *35*, 631−637.
(35) de Sousa, H. C. Ph.D. Thesis, New University of Lisbon, Lisbon, 1997.